Mean-field description of collapsing and exploding Bose-Einstein condensates

Sadhan K. Adhikari
Instituto de Física Teórica, Universidade Estadual Paulista, 01.405-900 São Paulo, São Paulo, Brazil

(Dated: February 1, 2008)

We perform numerical simulation based on the time-dependent mean-field Gross-Pitaevskii equation to understand some aspects of a recent experiment by Donley et al. on the dynamics of collapsing and exploding Bose-Einstein condensates of ^{85}Rb atoms. They manipulated the atomic interaction by an external magnetic field via a Feshbach resonance, thus changing the repulsive condensate into an attractive one and vice versa. In the actual experiment they changed suddenly the scattering length of atomic interaction from positive to a large negative value on a pre-formed condensate in an axially symmetric trap. Consequently, the condensate collapses and ejects atoms via explosion. We find that the present mean-field analysis can explain some aspects of the dynamics of the collapsing and exploding Bose-Einstein condensates.

PACS numbers: 03.75.Fi

I. INTRODUCTION

Recent successful detection [1, 2, 3] of Bose-Einstein condensates (BEC) in dilute bosonic atoms employing magnetic trap at ultra-low temperature has intensified experimental activities on various aspects of the condensate. On the theoretical front, numerical simulation based on the time-dependent nonlinear mean-field Gross-Pitaevskii (GP) equation [4] has provided a satisfactory account of some of these experiments [5, 6, 7, 8, 9]. Since the detection of BEC for ^{7}Li atoms with attractive interaction, one problem of extreme interest is the dynamical study of the formation and decay of BEC for attractive atomic interaction [3].

For attractive interaction the condensate is stable for a maximum critical number $N_{\rm cr}$ of atoms [3]. Measurements for $N_{\rm cr}$ [3, 10] are in reasonable agreement with the mean-field analyses for BEC of ^{7}Li in a spherically symmetric trap [5, 11], although there is some discrepancy for BEC of ^{85}Rb in an axially symmetric trap [12, 13]. If the number of atoms can somehow be increased beyond this critical number, due to interatomic attraction the condensate collapses emitting atoms until the number of atoms is reduced below $N_{\rm cr}$ and a stable configuration is reached. With a supply of atoms from an external source the condensate can grow again and thus a series of collapses can take place, that was observed experimentally in the BEC of ^{7}Li with attractive interaction [3]. Theoretical mean-field analysis has been able to explain this dynamics [5, 6, 7, 8, 9].

Recently a more challenging experiment has been performed by Donley et al. [14] at JILA on an attractive condensate of ^{85}Rb atoms [10] in an axially symmetric trap, where they manipulated the interatomic interaction by changing the external magnetic field exploiting a nearby Feshbach resonance [15]. In the vicinity of a Feshbach resonance the atomic scattering length a can be varied over a huge range by adjusting the external magnetic field. Consequently, they were able to change suddenly the atomic scattering length by a large amount for a BEC of ^{85}Rb atoms [10]. They even changed the sign of the scattering length, thus transforming a repulsive condensate into an attractive one. The original experiment on attractive ^{7}Li atoms [3] did not use a Feshbach resonance, hence the atomic interaction was fixed. This restricts the number of atoms in the ^{7}Li BEC to a number close to $N_{\rm cr}$ and the collapse is driven by a stochastic process [3, 14].

In the experiment conducted at JILA, Donley et al. changed a stable pre-formed repulsive condensate of ^{85}Rb atoms into a highly explosive and collapsing attractive condensate and studied the dynamics of collapsing and exploding condensates [14]. The natural scattering length of ^{85}Rb atoms is negative (attractive). By exploiting the Feshbach resonance they made it positive (repulsive) in the initial state, where the number of atoms, unlike in the experiment with ^{7}Li [3], could be arbitrarily large. So immediately after the jump in the scattering length to a large negative value, one has a highly unstable BEC, where the number of atoms could be much larger than $N_{\rm cr}$. Donley et al. have provided a quantitative estimate of the explosion of this BEC by measuring the number of atoms remaining in the condensate as a function of time until an equilibrium is reached. They claim that their experiment reveal many interesting phenomena that challenge theoretical models. Because the phenomenon looks very much like a tiny supernova, or exploding star, the researchers dubbed it a "Bosenova". The fundamental physical process underlying the explosion remains a mystery.

In this paper we perform a mean-field analysis based on the time-dependent GP equation to understand some aspects of the above collapse and explosion of the attractive condensate of ^{85}Rb atoms in an axially symmetric trap. To account for the loss of atoms from the strongly attractive condensate we include an absorptive nonlinear three-body recombination term in the GP equation. Three-body recombination leads to the formation of di-

atomic molecules with liberation of energy responsible for energetic explosion with ejection of matter from the BEC. This process could be termed "atomic fusion" in contrast to nuclear fusion in stars. The three-body recombination rate we use in numerical simulation is in agreement with previous experimental measurement [16] and theoretical calculation [17]. The numerical method, we use, for the solution of the time-dependent GP equation with an axially symmetric trap has appeared elsewhere [13, 18, 19]. We find that the present mean-field numerical simulation provides a fair description of some features of the experiment at JILA [14].

There have been other theoretical studies based on the mean-field GP equation [6, 7, 8, 9] to deal with dynamical collapse including an absorptive term to account for the loss of particles. In most cases the loss mechanism is three-body recombination as in the present study. However, Duine and Stoof [7] propose that the loss arises due to a new elastic process. Instead of attempting a full numerical solution of the GP equation with axial symmetry, these investigations used various approximations to study the time evolution of the condensate or employed a spherically symmetric trap. Duine and Stoof [7] consider the full anisotropic dynamics, but use a Gaussian approximation for the wave function rather than an exact numerical solution. Most of the other studies employed a spherically symmetric trap [6, 8]. However, the investigation of Ref. [9] employed an axially symmetric trap to describe some aspects of the experiment at JILA and we comment on this work in Sec. IV. In the present investigation we consider the complete numerical solution of the mean-field GP equation for an axially symmetric trap as in the experiment at JILA. It is realized that an approximate solution as in the previous studies can not explain the dynamics of this experiment [9, 14].

In Sec. II we present the theoretical model and the numerical method for its solution. In Sec, III we present our results that we compare with the experiment at JILA. Finally, in Secs. IV and V we present a brief discussion and concluding remarks.

II. NONLINEAR GROSS-PITAEVSKII EQUATION

A. Theoretical Model Equations

The time-dependent Bose-Einstein condensate wave function $\Psi(\mathbf{r};\tau)$ at position $\mathbf{r}$ and time τ allowing for atomic loss may be described by the following mean-field nonlinear GP equation [4, 5]

$$\left[-i\hbar\frac{\partial}{\partial\tau} - \frac{\hbar^2\nabla^2}{2m} + V(\mathbf{r}) + gN|\Psi(\mathbf{r};\tau)|^2 - \frac{i\hbar}{2} \times \left(K_2 N|\Psi(\mathbf{r};\tau)|^2 + K_3 N^2|\Psi(\mathbf{r};\tau)|^4\right)\right]\Psi(\mathbf{r};\tau) = 0 \quad (2.1)$$

Here m is the mass and N the number of atoms in the condensate, $g = 4\pi\hbar^2 a/m$ the strength of interatomic interaction, with a the atomic scattering length. A positive a corresponds to a repulsive interaction and a negative a to an attractive interaction. The terms K_2 and K_3 denote two-body dipolar and three-body recombination loss-rate coefficients, respectively. There are many ways to account for the loss mechanism [6, 7]. It is quite impossible to include them all in a self consistent fashion. Here we simulate the atom loss via the most important quintic three-body term K_3 [6, 8, 9]. The contribution of the cubic two-body loss term [16] is expected to be negligible [6, 9] compared to the three-body term in the present problem of the collapsed condensate with large density and will not be considered here.

The trap potential with cylindrical symmetry may be written as $V(\mathbf{r}) = \frac{1}{2}m\omega^2(r^2 + \lambda^2 z^2)$ where ω is the angular frequency in the radial direction r and $\lambda\omega$ that in the axial direction z. We are using the cylindrical coordinate system $\mathbf{r} \equiv (r, \theta, z)$ with θ the azimuthal angle. The normalization condition of the wave function is $\int d\mathbf{r}|\Psi(\mathbf{r};\tau)|^2 = 1$.

In the absence of angular momentum the wave function has the form $\Psi(\mathbf{r};\tau) = \psi(r, z;\tau)$. Now transforming to dimensionless variables defined by $x = \sqrt{2}r/l$, $y = \sqrt{2}z/l$, $t = \tau\omega$, $l \equiv \sqrt{\hbar/(m\omega)}$, and

$$\phi(x, y; t) \equiv \frac{\varphi(x, y; t)}{x} = \sqrt{\frac{l^3}{\sqrt{8}}}\psi(r, z;\tau), \quad (2.2)$$

we get

$$\left[-i\frac{\partial}{\partial t} - \frac{\partial^2}{\partial x^2} + \frac{1}{x}\frac{\partial}{\partial x} - \frac{\partial^2}{\partial y^2} + \frac{1}{4}\left(x^2 + \lambda^2 y^2 - \frac{4}{x^2}\right) + 8\sqrt{2}\pi n\left|\frac{\varphi(x, y; t)}{x}\right|^2 - i\xi n^2\left|\frac{\varphi(x, y; t)}{x}\right|^4\right]\varphi(x, y; t) = 0 \quad (2.3)$$

where $n = Na/l$ and $\xi = 4K_3/(a^2 l^4\omega)$. This scaled mean-field equation has the correct n dependence of the three-body term so that the same equation can be used to study the decay rate of different initial and final scattering lengths a_{initial} and a_{collapse}, respectively, and initial number of atoms N_0. In this study the term K_3 will be used for a description of atom loss in the case of attractive interaction, where the scattering length a is negative. From theoretical [20] and experimental [16] studies it has been found that for negative a, K_3 increases rapidly as $|a|^n$, where the theoretical study [20] favors $n = 2$ for smaller values of $|a|$. For larger $|a|$, a much larger rate of increase may take place [17, 20]. There are theoretical [17, 20, 21] and experimental [22] estimates of K_3 for ^{87}Rb, ^{23}Na, and ^{7}Li away from Feshbach resonance. However, no thorough and systematic study of the variation of K_3 near a Feshbach resonance has been performed [23]. An accurate representation of the variation of K_3 of ^{85}Rb near the Feshbach resonance is beyond the scope of this study and here we represent this variation via a

quadratic dependence: $K_3 \sim a^2$. This makes the parameter ξ above a constant for an experimental set up with fixed l and ω and in the present study we use a constant ξ.

The normalization condition of the wave function becomes

$$\mathcal{N}_{\rm norm} \equiv 2\pi \int_0^\infty dx \int_{-\infty}^\infty dy |\varphi(x,y;t)|^2 x^{-1} = 1. \quad (2.4)$$

For $K_3 = 0$, $\mathcal{N}_{\rm norm} = 1$, however, in the presence of loss $K_3 > 0$, $\mathcal{N}_{\rm norm} < 1$. The number of remaining atoms N in the condensate is given by $N = N_0 \mathcal{N}_{\rm norm}$, where N_0 is the initial number.

The root mean square (rms) sizes $x_{\rm rms}$ and $y_{\rm rms}$ are defined by

$$x_{\rm rms}^2 = \mathcal{N}_{\rm norm}^{-1} 2\pi \int_0^\infty dx \int_{-\infty}^\infty dy |\varphi(x,y;t)|^2 x, (2.5)$$

$$y_{\rm rms}^2 = \mathcal{N}_{\rm norm}^{-1} 2\pi \int_0^\infty dx \int_{-\infty}^\infty dy |\varphi(x,y;t)|^2 y^2 x^{-1} (2.6)$$

B. Numerical Detail

We solve the GP equation (2.3) numerically using a time-iteration method elaborated in Refs. [13, 18, 19, 24]. The full GP Hamiltonian is conveniently broken into three parts – H_x, H_y, and H_n – the first containing the x-dependent linear terms, the second containing the y-dependent linear terms and the third containing the nonlinear terms. The GP equations for the first two parts are defined on a two-dimensional set of grid points $N_x \times N_y$ using the Crank-Nicholson discretization method. The resultant tridiagonal equations along x and y directions are solved alternately by the Gaussian elimination method along the x and y directions [24]. The GP equation for the third part do not contain any space derivative and is solved essentially exactly. Effectively, each time iteration of the GP equation is broken up into three parts – using H_x, H_y and H_n. For a small time step Δ the error involved in this break-up procedure along x and y directions is quadratic in Δ and hence can be neglected. For numerical purpose we discretize the GP equation using time step $\Delta = 0.001$ and space step 0.1 for both x and y spanning x from 0 to 15 and y from -30 to 30. This domain of space was sufficient to encompass the whole condensate wave function even during and after collapse and explosion. The preparation of the initial repulsive wave function is now a routine job and was done by increasing the nonlinearity n of the GP equation (2.3) by 0.0001 in each time step Δ during time iteration starting with the known harmonic oscillator solution of Eq. (2.3) for $n = \xi = 0$ [13].

It is now appropriate to calculate the parameters of the present dimensionless GP equation (2.3) corresponding to the experiment at JILA. We follow the notation and nomenclature of Ref. [14]. Their radial and axial trap frequencies are $\nu_{\rm radial} = 17.5$ Hz and $\nu_{\rm axial} = 6.8$ Hz, respectively, leading to $\lambda = 0.389$. The harmonic oscillator length l of ^{85}Rb atoms for $\omega = 2\pi \times 17.5$ Hz and $m \approx 79176$ MeV is $l = \sqrt{\hbar/(m\omega)} = 26070$ Å. One unit of time t of Eq. (2.3) is $1/\omega$ or 0.009095 s. They prepared a stable ^{85}Rb condensate of $N_0 = 16000$ atoms with scattering length $a_{\rm initial} = 7a_0$, $a_0 = 0.5292$ Å, such that the initial $n = 2.274$. Then during an interval of time 0.1 ms the scattering length was ramped to $a = a_{\rm collapse} = -30a_0$ such that final $n = -9.744$. The final condensate is strongly attractive and unstable and undergoes a sequence of collapse and explosion.

The initial value of $n(= 2.274)$ was attained after 22740 time steps. The nonlinearity n is then ramped from 2.274 to -9.744 in 0.1 ms. As one unit of dimensionless time t is 0.009095 s, 0.1 ms corresponds to 11 steps of time Δ. In the present simulation, n is ramped from 2.274 to -9.744 in the GP equation by equal amount in 11 steps. The absorptive term ξ was set equal to zero during above time iteration. Now the system is prepared for the simulation of the collapse and explosion.

For the simulation of the collapse and explosion the cubic nonlinear term is maintained constant and a nonzero value of ξ is chosen. The time-evolution of the GP equation is continued as a function of time $t = \tau_{\rm evolve}$ starting at 0. The time-evolution is continued using time step $\Delta = 0.001$. After a small experimentation it is found that $\xi = 2$ fits the experiment at JILA satisfactorily. Unless otherwise specified, this value of ξ was used in all simulations reported in this paper for different $a_{\rm initial}$, $a_{\rm collapse}$, and N_0.

It is useful to compare this value of $\xi(= 2)$ with the experimental [16] and theoretical [20] estimates of three-body loss rate of ^{85}Rb. For this we recall that $K_3 = \xi a^2 l^4 \omega/4$. Under experimental condition of an external magnetic field of 250 gauss on ^{85}Rb [16] the scattering length was $a \sim -370a_0$. Consequently, the present value of $\xi(= 2)$ corresponds to $K_3 \simeq 9 \times 10^{-25}$ cm^6/s for $a \sim -370a_0$, which is about two times the experimental rate $K_3 = (4.24^{+0.70}_{-0.29} \pm 0.85) \times 10^{-25}$ cm^6/s [16] and about 1.3 times the theoretical rate $K_3 = 6.7 \times 10^{-25}$ cm^6/s at $a \sim -370a_0$ [17].

III. NUMERICAL RESULT

The numerical simulation using Eq. (2.3) with a nonzero ξ immediately yields the remaining number of atoms in the condensate after the jump in scattering length. The remaining number of atoms vs. time is plotted in Fig. 1 for $a_{\rm initial} = 7a_0$, $a_{\rm collapse} = -30a_0$, $\xi = 2$, and $N_0 = 16000$ and compared with the experimental data. In this figure we also plot the result in this case for $\xi = 3$, which leads to a better agreement with experiment for this specific case. However, the use of $\xi = 2$ leads to a more satisfactory overall agreement with experiment. Except this single curve in Fig. 1 and

the plot in Fig. 4 (a) below, which are calculated with $\xi = 3$, all results reported in this paper are calculated with $\xi = 2$.

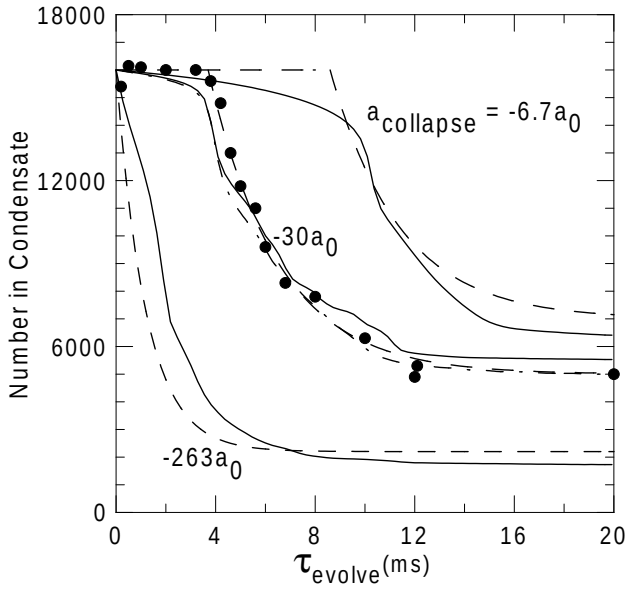

1.

FIG. 1: Number of remaining atoms in the condensate of 16000 ^{85}Rb atoms after ramping the scattering length from $a_{\rm initial} = 7a_0$ to $a_{\rm collapse} = -6.7a_0$, and $-30a_0$, $-263a_0$ in 0.1 ms as a function of evolution time $\tau_{\rm evolve}$ in ms. Solid circle: experiment for $a_{\rm collapse} = -30a_0$ [14]; full line: theory ($\xi = 2$); dash-dot line: theory ($\xi = 3$, $a_{\rm collapse} = -30a_0$); dashed line: average over preliminary, unanalized data using Eq. (3.1) [25].

In the experiment at JILA [14] it was observed that the strongly attractive condensate after preparation remains stable with a constant number of atoms for an interval of time $t_{\rm collapse}$, called collapse time. This behavior is physically expected. Immediately after the jump in scattering length from $7a_0$ to $-30a_0$, the attractive condensate shrinks in size during $t_{\rm collapse}$, until the central density increases to a maximum. Then the absorptive three-body term takes full control to initiate the explosion. Consequently, the number of atoms remains constant for $\tau_{\rm evolve} < t_{\rm collapse}$. The present result (full line) also shows a similar behavior. However, in this simulation the absorptive term is operative from $\tau_{\rm evolve} = 0$ and the atom number decreases right from beginning, albeit at a much smaller rate for $\tau_{\rm evolve} < t_{\rm collapse}$.

Donley et al. repeated their experiment with different values of $a_{\rm initial}$, $a_{\rm collapse}$, and N_0 [14]. For $a_{\rm initial} = 7a_0$ we repeated our calculation with the following values of final scattering length: $a_{\rm collapse} = -263a_0$ and $-6.7a_0$. These results are also plotted in Fig. 1 and agree with the unpublished, preliminary unanalyzed data [25]. The initial delay $t_{\rm collapse}$ in starting the explosion is large for small $|a_{\rm collapse}|$ as we see in Fig. 1. Similar effect was observed in the experiment for an initial condensate of 6000 atoms as shown in their Fig. 2 [14]. After a sequence of collapse and explosion, Donley et al. observed a "remnant" condensate of $N_{\rm remnant}$ atoms at large times containing a certain constant fraction of the initial N_0 atoms. Figure 1 shows such a behavior.

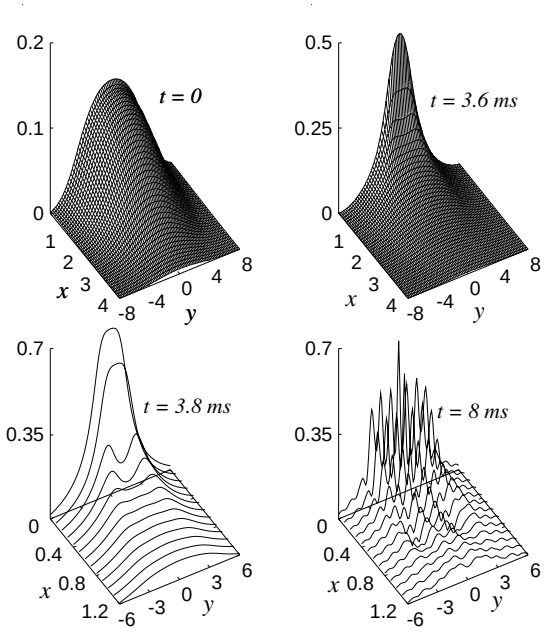

FIG. 2: The central part of the dimensionless wave function $|\phi(x,y)| \equiv |\varphi(x,y)/x|$ of the condensate on 0.1×0.1 grid for $\xi = 2$ after the jump in the scattering length of a BEC of 16000 ^{85}Rb atoms from $a_{\rm initial} = 7a_0$ to $a_{\rm collapse} = -30a_0$ at times $\tau_{\rm evolve} = 0$, 3.6 ms, 3.8 ms, and 8 ms. The quantities x and y are expressed in units of $l/\sqrt{2}$, where $l = 26070$ Å.

The above evolution of the condensate after the jump in scattering length to $-30a_0$ from $7a_0$ for $N_0 = 16000$ can be understood from a study of the wave function and we display the central part of the wave function in Fig. 2 for $\tau_{\rm evolve} = 0, 3.6, 3.8$, and 8 ms. The wave function immediately after jump at time $\tau_{\rm evolve} = 0$ is essentially the same as that before the jump at -0.1 ms. There is not enough time for the wave function to get modified at $\tau_{\rm evolve} = 0$. From Fig. 2 we find that at 3.6 ms the wave function is only slightly narrower than at 0 ms but still smooth and has not yet collapsed sufficiently. As $\tau_{\rm evolve}$ increases, the wave function contracts further and the explosion starts. At 3.8 ms some spikes (irregularities) have appeared in the wave function showing the beginning of the explosion and loss. From the study of the wave functions we find that the explosion start at $\tau_{\rm evolve} = t_{\rm collapse} \simeq 3.7$ ms in agreement with the experiment at JILA. We also find that at 3.7

ms before the loss began the bulk BEC did not contract dramatically as also observed in the experiment. In the numerical simulation for this case we find that at $\tau_{\rm evolve} = 0, x_{\rm rms} = 2.98\mu$m and $y_{\rm rms} = 4.21\mu$m and at $\tau_{\rm evolve} = 3.7$ ms, $x_{\rm rms} = 2.53\mu$m and $y_{\rm rms} = 4.10\mu$m. From Fig. 2 we see that at 8 ms the wave function is very spiky corresponding to the violent ongoing explosion.

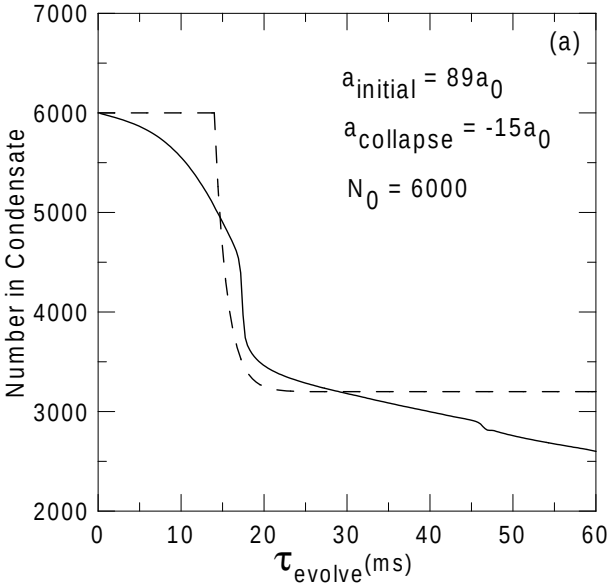

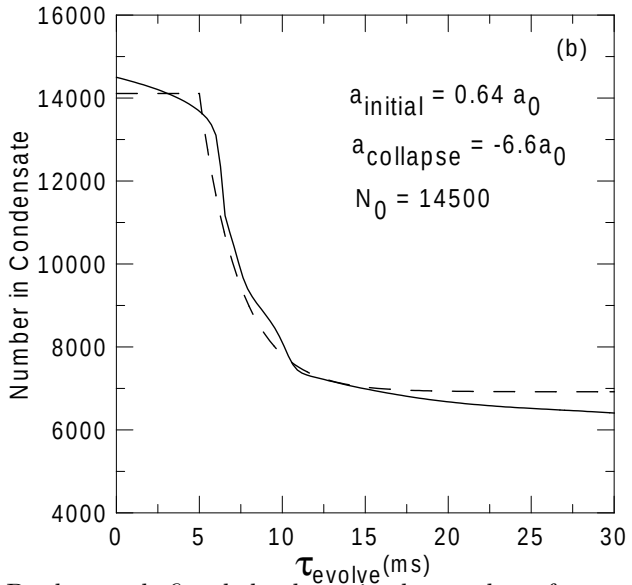

Donley et al. fitted the decay in the number of atoms during particle loss to a decay constant $\tau_{\rm decay}$ via the formula

$$N(\tau_{\rm evolve}) = N_{\rm remnant} + (N_0 - N_{\rm remnant}) \times e^{(t_{\rm collapse} - \tau_{\rm evolve})/\tau_{\rm decay}} \quad (3.1)$$

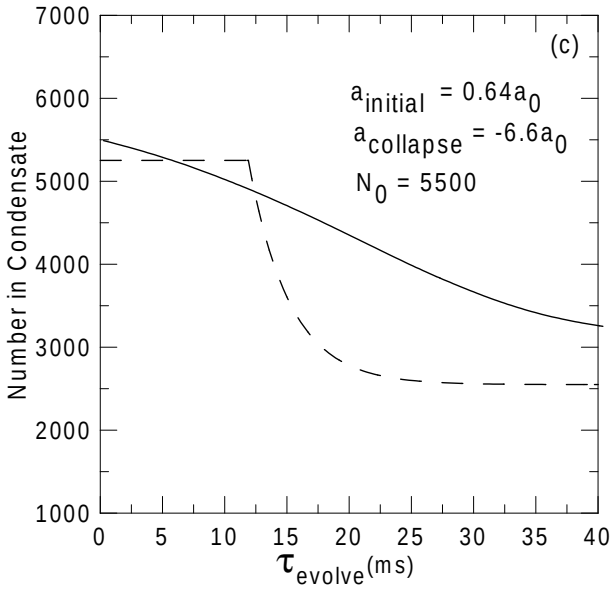

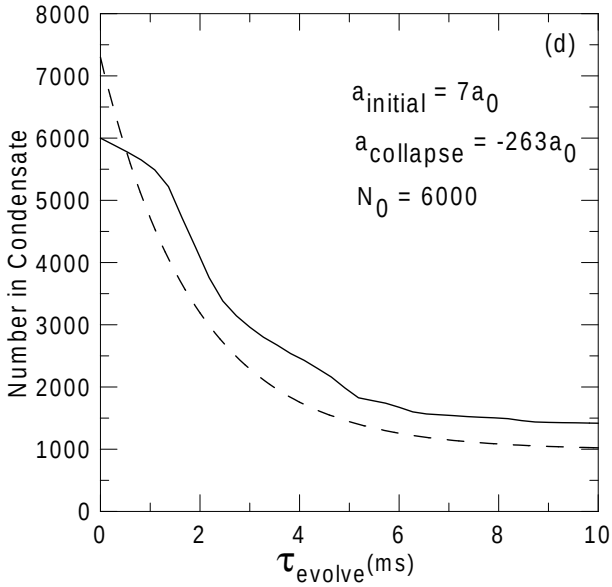

FIG. 3: More decay curves with $\xi = 2$ for (a) $a_{\rm initial} = 89a_0$, $a_{\rm collapse} = -15a_0$, and $N_0 = 6000$, (b) $a_{\rm initial} = 0.64a_0$, $a_{\rm collapse} = -6.6a_0$, and $N_0 = 14500$, (c) $a_{\rm initial} = 0.64a_0$, $a_{\rm collapse} = -6.6a_0$, and $N_0 = 5500$, and (d) $a_{\rm initial} = 7a_0$, $a_{\rm collapse} = -263a_0$, and $N_0 = 6000$. Full line: present theory; dashed line: average over preliminary, unanalyzed data using Eq. (3.1) [25].

for $\tau_{\rm evolve} > t_{\rm collapse}$. In Fig. 1 we also plot $N(\tau_{\rm evolve})$ of Eq. (3.1) (dashed line) for $a_{\rm collapse} = -263a_0, -30a_0$ and $-6.7a_0$ with respective decay rates $\tau_{\rm decay} = 1.2$ ms,

2.8 ms and 2.8 ms [25]. For wide variation of parameters $a_{\rm initial}, a_{\rm collapse}$, and N_0, $\tau_{\rm decay}$ varies approximately between 1 and 3. The results of the present simulation (full line) agree well with the average experimental result of Eq. (3.1) for three different $a_{\rm collapse}$ (dashed line) [25].

Next we repeated our calculation for several other values for $a_{\rm initial}$, $a_{\rm collapse}$, and N_0. These results are plotted in Fig. 3 for (a) $a_{\rm initial} = 89a_0$, $a_{\rm collapse} = -15a_0$, and $N_0 = 6000$, (b) $a_{\rm initial} = 0.64a_0$, $a_{\rm collapse} = -6.6a_0$, and $N_0 = 14500$, (c) $a_{\rm initial} = 0.64a_0$, $a_{\rm collapse} = -6.6a_0$, and $N_0 = 5500$, and (d) $a_{\rm initial} = 7a_0$, $a_{\rm collapse} = -263a_0$, and $N_0 = 6000$. The agreement of the result of simulation with unpublished, preliminary unanalyzed data is good in all four cases reported in Fig. 3 [25].

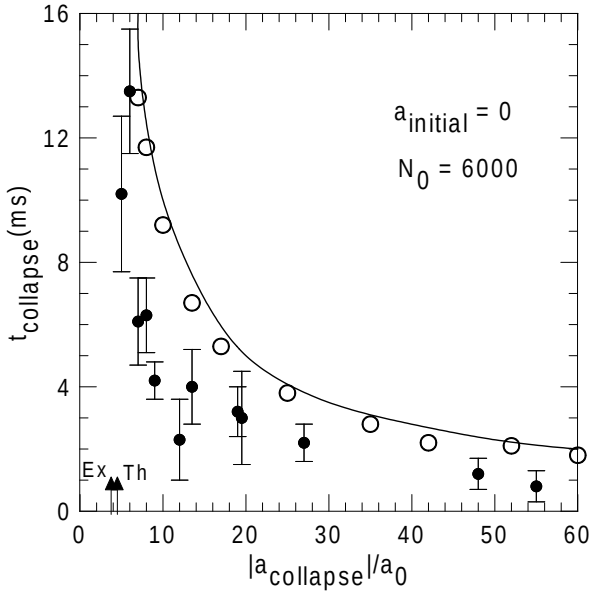

1.

FIG. 4: The collapse time $t_{\rm collapse}$ vs. $|a_{\rm collapse}|/a_0$ for $a_{\rm initial} = 0$, $N_0 = 6000$ and $\xi = 2$. Solid circle with error bar: experiment [14]; open circle: axially symmetric mean-field model of Ref. [9]; arrows marked Th and Ex are theoretical (4.49) [12, 13] and experimental (3.75) [10] estimates of $|a_{\rm collapse}|/a_0$, respectively, full line: present theory.

The decay curves in Fig. 3 are different, although they have certain general features which determine the decay constant $\tau_{\rm decay}$, collapse time $t_{\rm collapse}$, and number of atoms in the remnant. Experimentally, the fraction of atoms that went into the remnant decreased with $|a_{\rm collapse}|$ and was $\sim 40\%$ for $|a_{\rm collapse}| < 10a_0$ and was $\sim 10\%$ for $|a_{\rm collapse}| > 100a_0$. Figures 1 and 3 also show this behavior. The values of $\tau_{\rm decay}$ for plots in Figs. 3 (a) – (d) are 1.5 ms, 2.4 ms, 3.3 ms, and 1.9 ms, respectively, lying in the range $\sim 1 - 3$ ms [25]. The general features in the behavior of remnant number and collapse time are discussed in the following.

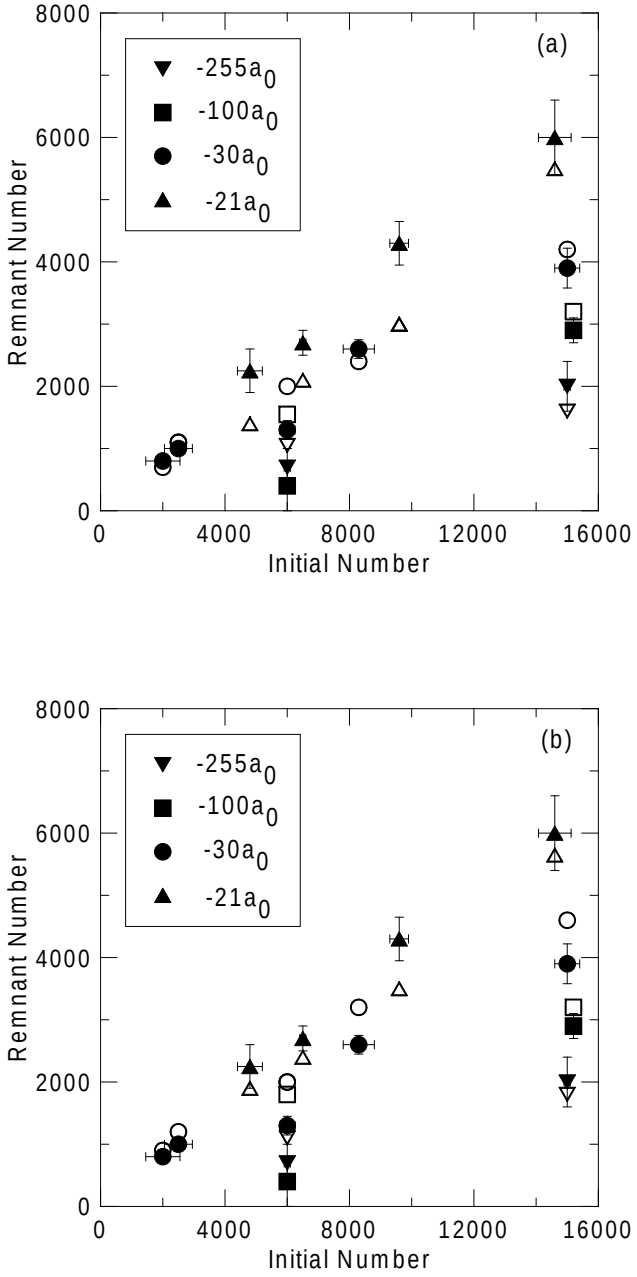

FIG. 5: Remnant number vs. initial number for $a_{\rm initial} = 7a_0$ and different $a_{\rm collapse}$ for (a) $\xi = 3$ and (b) $\xi = 2$. The experimental results [26] with error bars are represented by solid triangle, solid circle, solid square, and solid inverted triangle for $a_{\rm collapse} = -21a_0, -30a_0, -100a_0$ and $-255a_0$. The corresponding theoretical results are represented by open triangle, open circle, open square, and open inverted triangle.

Donley et al. provided a quantitative measurement of the variation of collapse time $t_{\rm collapse}$ with the final scattering length $a_{\rm collapse}$ for a given $a_{\rm initial} = 0$

and $N_0 = 6000$. We also calculated this variation using our model given by Eq. (2.3). In our calculation we define $t_{\rm collapse}$ as the time at which the spikes (irregularities), as in Fig. 2, tend to appear in the wave function. The results are plotted in Fig. 4 and compared with experimental data [14] as well as with another calculation using the mean-field GP equation in an axially symmetric trap [9]. The agreement between the two theoretical results is very good. There is also qualitative agreement between the experimental data on the one hand and the two calculations on the other hand: $t_{\rm collapse}$ decreases with $|a_{\rm collapse}|/a_0$ starting from an infinite value at $|a_{\rm collapse}| = a_{\rm cr}$ for a fixed N_0, that is 6000 in Fig. 4. For this N_0, $a_{\rm cr}$ is the minimum value of $|a_{\rm collapse}|$ that leads to the collapse and explosion. For a given N_0, a critical value of $n \equiv n_{\rm cr}$ for collapse can be defined via $n_{\rm cr} \equiv N_0 a_{\rm cr}/l$. As there is discrepancy between theoretical and experimental $n_{\rm cr}$ for an axially symmetric trap [12, 13], the theoretical and experimental $a_{\rm cr}$ are also supposed to be different. The experimental $k_{\rm cr} \equiv n_{\rm cr}\lambda^{1/6} = 0.46$ [10] and the theoretical $k_{\rm cr} = 0.55$ [12, 13] for the axially symmetric trap used in the experiment at JILA with the asymmetry parameter $\lambda = 0.389$. The theoretical $a_{\rm cr}$ should be larger than the experimental $a_{\rm cr}$ in the same proportion. This might imply that the theoretical $t_{\rm collapse}$ should tend to infinity for a slightly larger value of $a_{\rm collapse}$ as in Fig. 4.

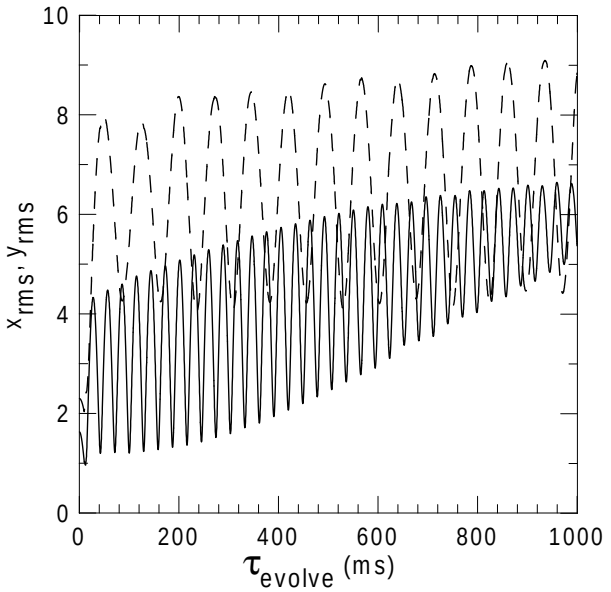

FIG. 6: The dimensionless rms sizes $x_{\rm rms}$ (full line) and $y_{\rm rms}$ (dashed line) expressed in units of $l/\sqrt{2}$ ($l = 26070$ Å) after the jump in the scattering length of a BEC of 16000 ^{85}Rb atoms from $a_{\rm initial} = 7a_0$ to $a_{\rm collapse} = -6.7a_0$ as functions of time $\tau_{\rm evolve}$ for $\xi = 2$.

Donley et al. measured the number of remnant atoms for $a_{\rm initial} = 7a_0$ and different initial number N_0 and $a_{\rm collapse}$ and these results [26] are plotted in Figs. 5 (a) and (b) and compared with numerical simulation performed with $\xi = 3$ and 2, respectively. The agreement is good for most cases shown in this figure. For $N_0 = 6000$, there is some discrepancy between theoretical and experimental remnant numbers. The overall agreement is better in the case with $\xi = 2$ than with $\xi = 3$. For $\xi = 3$ the three-body recombination loss-rate is larger and this leads to smaller remnant numbers compared to the case with $\xi = 2$. The theoretical $N_{\rm cr}$ for a fixed negative $a_{\rm collapse}$ is given by $N_{\rm cr} = 0.55 l\lambda^{-1/6}/|a_{\rm collapse}|$ [12, 13]. For $a_{\rm collapse} = -255a_0, -100a_0, -30a_0$, and $-21a_0$, $N_{\rm cr} = 124, 317, 1057$, and 1510, respectively. Hence, from Fig. 5 we find that the number in the remnant could be much larger than $N_{\rm cr}$ for times on the order of tens of milliseconds. However, in our simulation such a remnant continues to emit atoms at a much slower rate and for very large times on the order of seconds the number of atoms eventually tends towards $N_{\rm cr}$.

Donley et al. observed that the remnant condensate in all cases oscillated in a highly excited collective state with approximate frequencies $2\nu_{\rm axial}$ and $2\nu_{\rm radial}$ being predominantly excited. The actual measured frequencies are 13.6(6) Hz and 33.4(3) Hz. To find if this behavior emerges from the present simulation we plot in Fig. 6 sizes $x_{\rm rms}$ and $y_{\rm rms}$ vs. time for the condensate after the jump in the scattering length to $-6.7a_0$ from $7a_0$ for $N_0 = 16000$. Excluding the first 20 ms when the remnant condensate is being formed, we find a periodic oscillation in $x_{\rm rms}$ and $y_{\rm rms}$ with frequencies 13.5 Hz and 34 Hz, respectively, as observed in experiment.

IV. DISCUSSION

Though we have explained some aspects of the experiment at JILA, certain detailed features have not been addressed in this study. Donley et al. have classified the emitted atoms in three categories: burst, missing (undetected) and jet atoms [14]. The jet atoms appear with much lower energy solely in the radial direction possibly from the spikes in the wave function when the collapse is suddenly interrupted during the period of atom loss before the remnant is formed. Strangely enough the emission of jet atoms are found not to possess axial symmetry always and hence can not be properly treated in a axially symmetric model. Moreover a clear-cut distinction between the burst and missing atoms emitted during the explosion seems to be difficult in the present model as the experiment could not specify the properties (magnitude and direction of velocities) of the missing atoms. Also, because of the missing atoms it is difficult to predict the energy distribution of the burst atoms during the explosion in a mean-field analysis. Without proper identification of the missing atoms, any energy distribution calculated using the present mean-field analysis will yield the total energy of burst plus missing atoms. A careful

1.

analysis of the energy of the emitted atoms is required for explaining the exclusive features and a detailed study of the wave function is needed for this purpose. Such an analysis is beyond the scope of the present investigation and would be a welcome future theoretical work.

The success of the Crank-Nicholson algorithm in alternate directions as used in this study depends on a proper discretization of the GP equation in space and time. In this study we employed a two-dimensional lattice in space of 600×150 or 90000 points ($x \leq 15, -30 \leq y \leq 30$) and a time step of 0.001. In the absence of collapse and recombination loss this discretization leads to very precise results. The accuracy reduces in the presence of the violent collapse and explosion simulated by three-body recombination. By varying the space discretization grid and time step we found that the estimated error in the present calculation is less than $\sim 10\%$ for time propagation upto few tens of milliseconds.

There has been another attempt to use the mean-field GP equation in an axially symmetric trap [9] to explain the experiment of Ref. [14]. There are certain differences between the analysis of Ref. [9] and the present investigation. According to the experiment of Ref. [14], the burst atoms and missing atoms are components of expelled atoms which lose contact with the central condensate that eventually forms the remnant. Of these the burst atoms have energy much less than the magnetic trap depth. Hence, though expelled from the central condensate they continue trapped and oscillate with time. The wave function of Eq. (2.3) only describes the central condensate. However, in Ref. [9] the burst atoms are considered to be the peripheral part (the spikes) of the central condensate and hence taken to be described by the mean-field Eq. (2.3). The missing atoms are actually parts of the expelled atoms that have disappeared from the trap [14]. In Ref. [9], the missing atoms have been taken to be the only component of the emitted atoms. These are the main differences between the point of view of the present analysis and that of Ref. [9].

The three-body loss rates of the two studies are also widely different. Here we employ the three-body recombination loss-rate $K_3 \simeq 9 \times 10^{-25}$ cm^6/s for $a = -370a_0$ whereas in Ref. [9] the value $K_3 \sim 10^{-28}$ cm^6/s has been considered. The present rate is in rough agreement with the experimental rate of Ref. [16] ($K_3 \sim 4.2 \times 10^{-25}$ cm^6/s) and with the theoretical rate of Ref. [17] ($K_3 \sim 6.7 \times 10^{-25}$ cm^6/s) for the same value of scattering length whereas that of Ref. [9] is orders of magnitude smaller. However, such a small three-body rate in Ref. [9] has led to a large residual condensate at large time that they have interpreted as the sum of burst plus remnant. The use of a large three-body rate in this study has led to a much smaller residual central condensate which has been identified as the remnant as in the experiment at JILA [14].

However, it is assuring to see that the $t_{\rm collapse}$ vs. $|a_{\rm collapse}|/a_0$ curve of the two models in Fig. 4 agrees with each other. The present calculation in Fig. 4 was performed with a nonzero loss rate K_3, whereas that in Ref. [9] was performed by setting $K_3 = 0$. We find that K_3 plays an insignificant role in this calculation at small times. Hence, the two computer routines lead to the same result in the absence of recombination loss before the beginning of the explosion.

V. CONCLUSION

In conclusion, we have employed a numerical simulation based on the accurate solution [13] of the mean-field Gross-Pitaevskii equation with a cylindrical trap to study the dynamics of the collapse and explosion as observed in the recent experiment at JILA [14]. In the GP equation we include a quintic three-body nonlinear recombination loss term that accounts for the decay of the strongly attractive condensate. The results of the present simulation accounts for some aspects of the experiment.

In the experiment a strongly attractive ^{85}Rb condensate was prepared by ramping the scattering length to a large negative value and the subsequent decay of the collapsing and exploding condensate was measured. We have been able to understand the following features of this dynamics from the present numerical simulation: (1) The condensate undergoes collapse and explosion and finally stabilizes to a remnant condensate containing about $\sim 10\%$ (for $|a_{\rm collapse}| > 100a_0$) to 40% (for $|a_{\rm collapse}| < 10a_0$) of initial number of atoms N_0 at large times. This percentage is independent of N_0 and the ramped scattering length $a_{\rm collapse}$. The number in the remnant condensate can be much larger than the critical number for collapse $N_{\rm cr}$ for the same atomic interaction for experimental times on the order of tens of milliseconds. (2) Both in the experiment and our simulation the remnant condensate executes radial and axial oscillations in a highly excited collective state for a long time with frequencies $2\nu_{\rm radial}$ and $2\nu_{\rm axial}$. (3) After the sudden change in the scattering length to a large negative value, the condensate needs an interval of time $t_{\rm collapse}$ before it experiences loss via explosion. Consequently, the decay starts after the interval of time $t_{\rm collapse}$. (4) The number of atoms in the condensate decays exponentially with a decay constant $\tau_{\rm decay}$ of few milliseconds ($\sim 1-3$ ms).

To conclude, a large part of the Bosenova experiment on ^{85}Rb atoms at JILA [14], specially the detailed behavior of the remnant, can be understood by introducing the rather conventional three-body recombination loss in the standard mean-field GP equation, with a loss rate compatible with other studies [16, 17]. The study of the detailed behavior of the burst and missing atoms and the formation of the jet in such a mean-field theory seems to be more complicated technically, nevertheless viable, and would be a subject of future investigation.

Acknowledgments

The author extends sincere thanks to Dr. E. A. Donley for additional unpublished data [25, 26] of the experiment at JILA [14]. The work is supported in part by the CNPq and FAPESP of Brazil.

[1] M. H. Anderson, J. R. Ensher, Jr., M. R. Matthews, C. E. Wieman, E. A. Cornell, Science **269**, 198 (1995); J. R. Ensher, D. S. Jin, M. R. Matthews, C. E. Wieman, and E. A. Cornell, Phys. Rev. Lett. **77**, 4984 (1996); K. B. Davis, M. O. Mewes, M. R. Andrews, N. J. van Druten, D. S. Durfee, D. M. Kurn, and W. Ketterle, *ibid.* **75**, 3969 (1995); D. G. Fried, T. C. Killian, L. Willmann, D. Landhuis, S. C. Moss, D. Kleppner, T. J. Greytak, *ibid.* **81**, 3811 (1998).

[2] A. Robert, O. Sirjean, A. Browaeys, J. Poupard, S. Nowak, D. Boiron, C. I. Westbrook, and A. Aspect, Science **292**, 461 (2001); F. Pereira Dos Santos, J. Léonard, J. Wang, C. J. Barrelet, F. Perales, E. Rasel, C. S. Unnikrishnan, M. Leduc, and C. Cohen-Tannoudji, Phys. Rev. Lett. **86**, 3459 (2001); G. Modugno, G. Ferrari, G. Roati, R. J. Brecha, A. Simoni, and M. Inguscio, Science **294**, 1320 (2001).

[3] J. M. Gerton, D. Strekalov, I. Prodan, and R. G. Hulet, Nature **408**, 692 (2001); C. C. Bradley, C. A. Sackett, J. J. Tollett, and R. G. Hulet, Phys. Rev. Lett. **75**, 1687 (1995); C. C. Bradley, C. A. Sackett, and R. G. Hulet, *ibid.* **78**, 985 (1997).

[4] E. P. Gross, Nuovo Cimento **20**, 454 (1961); L. P. Pitaevskii, Zh. Eksp. Teor. Fiz. **40**, 646 (1961)[Sov. Phys. JETP **13**, 451 (1961)]; A. J. Leggett, Rev. Mod. Phys. **73**, 307 (2001).

[5] F. Dalfovo, S. Giorgini, L. P. Pitaevskii, and S. Stringari, Rev. Mod. Phys. **71**, 463 (1999).

[6] H. Saito and M.Ueda, Phys. Rev. A **63**, 043601 (2001); Phys. Rev. Lett. **86**, 1406 (2001); A. Eleftheriou and K. Huang, Phys. Rev. A **61**, 043601 (2000).

[7] R. A. Duine and H. T. C. Stoof, Phys. Rev. Lett. **86**, 2204 (2001).

[8] Y. Kagan, A. E. Muryshev, and G. V. Shlyapnikov, Phys. Rev. Lett. **81**, 933 (1998); Y. Kagan, E. L. Surkov, and G. V. Shlyapnikov, *ibid.* **79**, 2604 (1997); A. Gammal, T. Frederico, L. Tomio, and Ph. Chomaz, Phys. Rev. A **61**, 051602 (2000); M. Ueda and K. Huang, *ibid.* **60**, 3317 (1999).

[9] H. Saito and M. Ueda, Phys. Rev. A **65**, 033624 (2002).

[10] J. L. Roberts, N. R. Claussen, S. L. Cornish, E. A. Donley, E. A. Cornell, and C. E. Wieman, Phys. Rev. Lett. **86**, 4211 (2001); S. L. Cornish, N. R. Claussen, J. L. Roberts, E. A. Cornell, and C. E. Wieman, *ibid.* **85**, 1795 (2000).

[11] R. J. Dodd, M. Edwards, C. J. Williams, C. W. Clark, M. J. Holland, P. A. Ruprecht, and K. Burnett, Phys. Rev. A **54**, 661 (1996); F. Dalfovo and S. Stringari, *ibid.* **53**, 2477 (1996); M. Houbiers and H. T. C. Stoof, *ibid.* **54**, 5055 (1996); A. Gammal, T. Frederico, and L. Tomio, Phys. Rev. E **60**, 2421 (1999).

[12] A. Gammal, T. Frederico, and L. Tomio, Phys. Rev. A **64**, 055602 (2001).

[13] S. K. Adhikari, Phys. Rev. E **65**, 016703 (2002).

[14] E. A. Donley, N. R. Claussen, S. L. Cornish, J. L. Roberts, E. A. Cornell, and C. E. Wieman, Nature **412**, 295 (2001).

[15] S. Inouye, M. R. Andrews, J. Stenger, H. J. Miesner, D. M. Stamper-Kurn, and W. Ketterle, Nature **392**, 151 (1998); Ph. Courteille, R. S. Freeland, D. J. Heinzen, F. A. van Abeelen, and B. J. Verhaar, Phys. Rev. Lett. **81**, 69 (1998); V. Vuletić, A. J. Kerman, C. Chin, and S. Chu, *ibid.* **82**, 1406 (1999); E. Timmermans, P. Tommasini, M. Hussein, and A. Kerman, Phys. Rep. **315**, 199 (1999).

[16] J. L. Roberts, N. R. Claussen, S. L. Cornish, and C. E. Wieman, Phys. Rev. Lett. **85**, 728 (2000).

[17] B. D. Esry, C. H. Greene, and J. P. Burke, Jr., Phys. Rev. Lett. **83**, 1751 (1999).

[18] S. K. Adhikari, Phys. Rev. E **62**, 2937 (2000); **63**, 056704 (2001); Phys. Rev. A **63**, 043611 (2001); **65**, 033616 (2002).

[19] M. Holland and J. Cooper, Phys. Rev. A **53**, R1954 (1996); F. Dalfovo and M. Modugno, *ibid.* **61**, 023605 (2000); P. A. Ruprecht, M. J. Holland, K. Burnett, and M. Edwards, *ibid.* **51**, 4704 (1995); B. I. Schneider and D. L. Feder, *ibid.* **59**, 2232 (1999); M. M. Cerimele, M. L. Chiofalo, F. Pistella, S. Succi, and M. P. Tosi, Phys. Rev. E **62**, 1382 (2000).

[20] A. J. Moerdijk, H. M. J. M. Boesten, and B. J. Verhaar, Phys. Rev. A **53**, 916 (1996).

[21] J. M. Gerton, C. A. Sackett, B. J. Frew, and R. G. Hulet, Phys. Rev. A **59**, 1514 (1999); E. A. Burt, R. W. Ghrist, C. J. Myatt, M. J. Holland, E. A. Cornell, and C. E. Wieman, Phys. Rev. Lett. **79**, 337 (1997); D. M. Stamper-Kurn, M. R. Andrews, A. P. Chikkatur, S. Inouye, H. -J. Miesner, J. Stenger, and W. Ketterle, *ibid.* **80**, 2027 (1998).

[22] P. O. Fedichev, M. W. Reynolds, and G. V. Shlyapnikov, Phys. Rev. Lett. **77**, 2921 (1996).

[23] E. Braaten and H. W. Hammer, Phys. Rev. Lett. **87**, 160407 (2001); P. F. Bedaque, E. Braaten, and H. W. Hammer, *ibid.* **85**, 908 (2000).

[24] S. E. Koonin and D. C. Meredith, *Computational Physics Fortran Version* (Addison-Wesley, Reading, 1990), pp 169-180.

[25] E. A. Donley, *private communication* (2001), Donley kindly made the preliminary and unanalized, nevertheless, very useful unpublished data for particle loss presented in Figs. 1 and 3 available (however, not shown in these figures) and checked that the results of our numerical simulation for all the cases presented in these figures agree well with the unpublished data.

[26] E. A. Donley, *private communication* (2001); E. A. Donley, N. R. Claussen, S. L. Cornish, J. L. Roberts, E. A. Cornell, and C. E. Wieman, to be published.